IEEE Access
Multidisciplinary | Rapid Review | Open Access Journal

Received April 16, 2020, accepted May 3, 2020, date of publication May 11, 2020, date of current version May 22, 2020.

Digital Object Identifier 10.1109/ACCESS.2020.2993246

Environment-Aware Coverage Optimization for Space-Ground Integrated Maritime Communications

TE WEI[1,2], (Student Member, IEEE), WEI FENG[1,2], (Senior Member, IEEE), NING GE[1,2], (Member, IEEE), AND JIANHUA LU[1,2], (Fellow, IEEE)

[1]Department of Electronic Engineering, Tsinghua University, Beijing 100084, China
[2]Beijing National Research Center for Information Science and Technology, Tsinghua University, Beijing 100084, China

Corresponding author: Wei Feng (fengwei@tsinghua.edu.cn)

This work was supported in part by the National Key Research and Development Program of China under Grant 2018YFA0701601, in part by the National Natural Science Foundation of China under Grant 61771286, Grant 61922049, Grant 61941104, and Grant 61701457, in part by the Nantong Technology Program under Grant JC2019115, and in part by the Beijing Innovation Center for Future Chip.

ABSTRACT To satisfy the growing demand for broadband maritime communications, space-ground integrated maritime communication networks (MCNs) arise, which are envisioned to take full advantage of both satellites and terrestrial shore-based networks. In practice, due to the frequent beam hopping of satellites and the limited number of geographically available onshore base-station sites, the space-ground integrated MCN usually presents a highly non-cellular network structure, leading to both challenging blind zones and coverage areas with severe interference. In this paper, we optimize the coverage performance by exploiting the marine environment information. Particularly, the transmit antenna correlation is estimated using the location and mobility information of scatterers on the sea, such as lighthouses, reefs, islands, and vessels. The position and attitude information of satellites are also utilized for interference estimation. Based on that, we optimize the input covariance and precoding matrix to maximize the ergodic sum capacity for all mobile terminals within the coverage. It is a complicated non-convex problem, especially because the ergodic sum capacity is difficult to be expressed straightly without the expectation operator. We introduce an upper bound of the ergodic sum capacity using the path loss and the transmit antenna correlation estimated from the environment information, and then propose an iterative algorithm to solve the problem by solving a set of convex subproblems. The proposed environment-aware scheme is evaluated using the real-world geographic information of a coastal area of China. Simulation results demonstrate that the proposed scheme can greatly improve the ergodic sum capacity and the energy efficiency compared with existing approaches, and achieve dynamic coverage to match the non-cellular network structure.

INDEX TERMS Maritime communications, marine environment information, non-cellular, coverage optimization, dynamic coverage.

I. INTRODUCTION

With the rapid development of marine industries, such as marine tourism, offshore aquaculture and oceanic mineral exploration, there is a growing demand for broadband maritime communication services [1]. Satellites have large coverage areas to enable global maritime communications, but most of them offer currently only narrowband services, e.g., a maximum rate of 492 kbps provided by the widely-used international maritime satellites (Inmarsat). Besides, although some high-throughput satellites have been being planned, high-power transmitters and high-sensitivity receivers are always required for satellite terminals (STs) to overcome the high propagation loss [2]. On the ground side, by setting up base stations (BSs) along the coast, the shore-based maritime communication network (MCN) can provide broadband services for coastwise mobile terminals (MTs). However, its coverage area is usually limited. The farthest coverage distance reported in the literature is only 100 km, which even cannot support maritime activities in the exclusive economic zone (EEZ) [3]. Therefore, it is of great interest to build a space-ground integrated network for maritime

The associate editor coordinating the review of this manuscript and approving it for publication was Zhenyu Zhou.

communications, so as to achieve the coordination gain, taking full advantage of both satellites and shore-based networks [4].

Due to the limited number of geographically available onshore BS sites, and the strong mobility of low-Earth orbit (LEO) and medium-Earth orbit (MEO) satellites, the space-ground integrated MCN has a highly non-cellular structure, which is different from terrestrial cellular networks. As a result, there always exist blind zones despite of network planning. In addition, when a terrestrial BS covers the MTs far from shore with high power, it will inevitably cause strong co-channel interference to the close-range MTs served by the neighboring BSs, as well as the STs nearby [5]. The ergodic sum capacity is often restricted by the blind zones and the coverage areas with severe interference, posing great challenges to the design of practical MCNs. Therefore, it is critically important to reconsider the coverage optimization issue for space-ground integrated MCNs [6].

Generally, the coverage performance of space-ground integrated networks can be optimized with the cooperative design of signals transmitted by different BSs. In [7], the authors optimized the deployment of BSs and analyzed the gain of directional beamforming. In [8], a cognitive spectrum sharing and frequency reuse scheme was proposed to improve inter-cell fairness. More recently, the authors of [9] proposed a beamforming scheme based on the uplink-downlink duality theory to decrease the co-channel interference. These studies all require full channel state information (CSI) at the transmitter. To reduce the overhead of acquiring CSI, the authors in [10] exploited large-scale CSI instead of full CSI for coverage optimization. All of the above schemes, however, have not fully utilized the wireless propagation environment information, such as the geographic location of scatterers, due to the complicated distribution pattern and unpredictable movement of the scatterers.

Different from terrestrial networks, geographical environment characteristics could be exploited for coverage optimization in the MCN. Previous channel modeling studies have suggested that maritime channels consist of only a few strong propagation paths due to the limited number of scatterers [11]. Some scatterers mounted in fixed locations, such as the lighthouses, reefs, and islands, can be observed using remote sensing techniques [12]. Besides, the locations of moving scatterers such as vessels and sea waves can be estimated using vessel detectors for maritime surveillance [13] and the trochoid model [14], respectively. Therefore, the transmit antenna correlation can be acquired from the marine environment, such as the azimuth angle between the scatterers and the transmit antennas.

In this paper, we optimize the coverage performance of the MCN using the path loss and the transmit antenna correlation estimated from the environmental information, i.e., the location and mobility information of scatterers. For all the MTs within the coverage, the ergodic sum capacity is maximized by optimizing the input covariance and the precoding matrix, while providing the STs with guaranteed quality of service (QoS). We derive the correlation matrix from the azimuth angle of departure (AoD) of each scattering path, and express the ergodic sum capacity without the small-scale CSI. The optimization problem is proved a complicated non-convex one. We introduce a tight upper bound to approximate the ergodic sum capacity, and propose an iterative algorithm to solve the problem by solving a convex subproblem in each iteration. We evaluate the performance of the proposed environment-aware scheme using Matlab and Visualyse, where the real-world geographic information of a coastal area around the Chongming Island of China is used to estimate the CSI. Simulation results reveal that the proposed scheme can greatly improve the ergodic sum capacity and achieve dynamic coverage for the non-cellular space-ground integrated MCN. The main contributions of this paper are summarized as follows:

- An environment-aware MCN structure is proposed, where the information of marine environment is collected and used for more precise channel estimation.
- Using the environmental information, a cooperative coverage optimization algorithm is proposed for the space-ground integrated MCN. The ergodic sum capacity of all the MTs within the coverage is maximized, while the STs are provided with guaranteed QoS.
- The performance of the proposed scheme is evaluated using the real-world geographic information of a coastal area of China. The impact of BS configuration and network topology on the coverage performance is also discussed.

The remainder of this paper is organized as follows: Section II introduces the system model of an environment-aware space-ground integrated MCN. In Section III, the formulation of the cooperative coverage optimization problem is presented, and an iterative algorithm is proposed to solve the problem. Section IV presents simulation results and further discussions. Finally, Section V concludes this paper.

Throughout this paper, lightface symbols represent scalars, while boldface symbols denote vectors and matrices. $\mathcal{C}^{M\times N}$ represents an $M \times N$ complex matrix, and $\mathcal{CN}(0, \sigma^2)$ denotes the complex Gaussian distribution with zero mean and σ^2 variance. $\mathbf{I}_N$ represents an $N \times N$ identity matrix, and $\mathbf{O}$ denotes a zero matrix. $[\mathbf{A}]_{(p,q)}$ represents the element in the p-th row and the q-th column of $\mathbf{A}$. $diag\{\mathbf{A}_1, \ldots, \mathbf{A}_N\}$ denotes a block diagonal matrix composed by $\mathbf{A}_1, \ldots, \mathbf{A}_N$. $|a|$ represents the magnitude of a. $\mathbf{A}^H$ denotes the transpose conjugate of $\mathbf{A}$. $\mathbb{E}(\cdot)$, $det(\cdot)$ and $tr(\cdot)$ represent the expectation operator, the determinant operator and the trace operator, respectively.

II. SYSTEM MODEL

As depicted in Fig. 1, we consider the downlink transmission of a frequency division duplexing MCN consisting of K onshore BSs. Each BS k $(k = 1, 2, \ldots, K)$ consists of N_k correlated antenna arrays (CAAs) equipped with L antenna

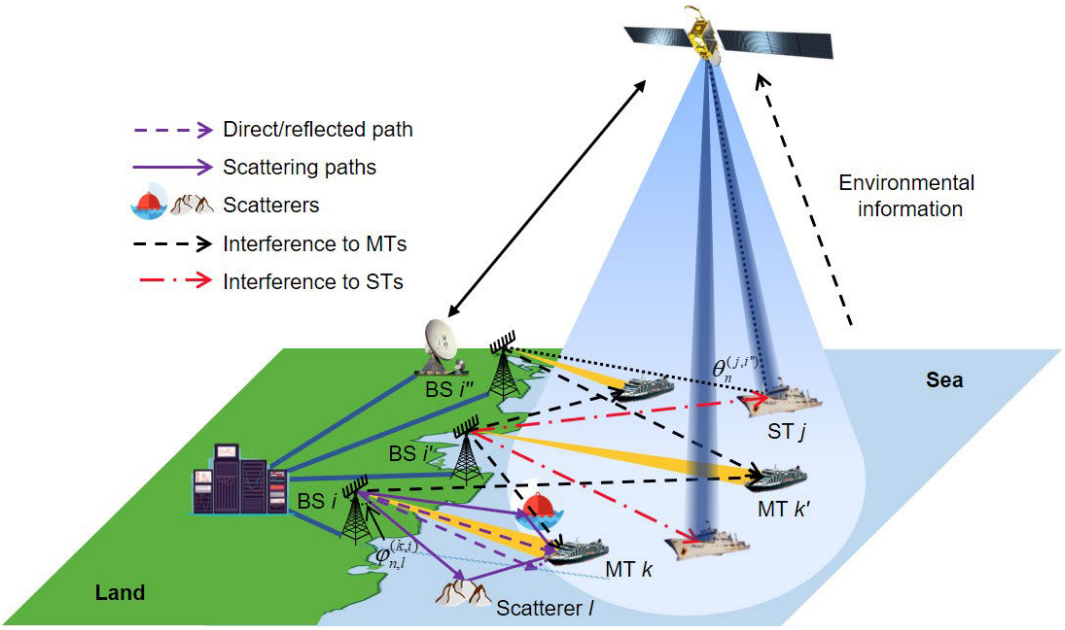

FIGURE 1. A space-ground integrated MCN, where environmental information is collected via narrowband wide-area communication systems (e.g. satellites), and utilized for coverage optimization. The environmental information, such as the scatterer locations and the satellite attitude, as well as the corresponding channel parameters, are depicted for MT *k* and ST *j* as an example. For simplicity, the interference from BS *i'* and the interference to MT *k'* are depicted as an illustration of co-channel interference, while the other interference paths are not shown.

elements, serving a MT equipped with M_k antenna elements. There are also J STs suffering co-channel interference.

We propose an environment-aware MCN structure to achieve dynamic coverage, as depicted in Fig. 2. The information of marine environment is gathered via a signalling network, where the locations of fixed scatterers (such as lighthouses, reefs and islands) are obtained from remote sensing satellites, and the locations of moving scatterers (such as vessels) are estimated using vessel detectors and shipping lanes. Using the environmental information, BSs can then estimate the CSI (e.g. the path loss and the transmit antenna correlation) and generate dynamic beams accordingly, user terminals with directional antennas can also adjust the antenna patterns to match the desired signals.

The received signal of the k-th MT can be expressed as

$$\mathbf{y}^{(k)} = \mathbf{H}^{(k,k)}\mathbf{x}^{(k)} + \sum_{i=1,\, i\neq k}^{K} \mathbf{H}^{(k,i)}\mathbf{x}^{(i)} + \mathbf{n}^{(k)} \tag{1}$$

where $\mathbf{H}^{(k,i)} \in \mathcal{C}^{M_k \times N_i L}$ is the channel gain from the i-th ($i = 1, 2, \ldots, K$) BS to the k-th MT, and $\mathbf{n}^{(k)} \sim \mathcal{CN}(0, \sigma^2 \mathbf{I}_{M_k})$ denotes the receiver noise. In a practical shore-based MCN, large antenna arrays are always equipped at the BSs to extend the range of coverage, and hybrid precoding can be used instead of full digital precoding to reduce the hardware cost and complexity. Therefore, the transmitted signal for the i-th MT $\mathbf{x}^{(i)} \in \mathcal{C}^{N_i L}$ can be written as

$$\mathbf{x}^{(i)} = \mathbf{w}^{(i)}\mathbf{b}^{(i)}s^{(i)} \tag{2}$$

where $s^{(i)}$ is the normalized transmitted symbol, $\mathbf{b}^{(i)}$ and $\mathbf{w}^{(i)}$ are the baseband precoding matrix and the radio frequency (RF) precoding matrix, respectively. Each element of $\mathbf{w}^{(i)}$ satisfies the magnitude constraint $\left|\left[\mathbf{w}^{(i)}\right]_{(p,q)}\right| = \frac{1}{\sqrt{N_i L}}$. We assume a total transmit power constraint $P_{\max}^{(k)}$ for each BS k, i.e.,

$$tr\left(\mathbb{E}\left[\mathbf{x}^{(k)}\mathbf{x}^{(k)H}\right]\right) = tr\left(\mathbf{\Phi}^{(k)}\right) \leq P_{\max}^{(k)} \tag{3}$$

where $\mathbf{\Phi}^{(k)} = \mathbf{w}^{(k)}\mathbf{b}^{(k)}\mathbf{b}^{(k)H}\mathbf{w}^{(k)H}$ is the input covariance for the k-th MT.

Generally, $\mathbf{H}^{(k,i)}$ can be expressed as [15]

$$\mathbf{H}^{(k,i)} = \mathbf{S}^{(k,i)}\mathbf{T}^{(k,i)^{1/2}}\mathbf{L}^{(k,i)}. \tag{4}$$

$\mathbf{S}^{(k,i)} \in \mathcal{C}^{M_k \times N_i L}$ is the small-scale fading matrix, whose entries follow independent and identical distribution $\mathcal{CN}(\mathbf{0}, 1)$. $\mathbf{T}^{(k,i)} \in \mathcal{C}^{N_i L \times N_i L}$ denotes the transmit antenna correlation matrix. The path loss $\mathbf{L}^{(k,i)} \in \mathcal{C}^{N_i L_i \times N_i L_i}$ can be modeled as

$$\mathbf{L}^{(k,i)} = diag\left\{l_1^{(k,i)}\mathbf{I}_{L_i}, \ \ldots, \ l_{N_i}^{(k,i)}\mathbf{I}_{L_i}\right\} \tag{5}$$

with the average propagation loss $l_n^{(k,i)}$ ($n = 1, 2, \ldots, N_i$) satisfying [11]

$$l_n^{(k,i)} = \left(\frac{\lambda}{4\pi d_n^{(k,i)}}\right)\left|2\sin\left(\frac{2\pi h_t^{(i)} h_r^{(k)}}{\lambda d_n^{(k,i)}}\right)\right| g\left(\theta_n^{(k,i)}\right) \tag{6}$$

where λ denotes the carrier wavelength, $d_n^{(k,i)}$ is the distance between the n-th CAA of the i-th BS and the k^{th} MT, $h_t^{(i)}$

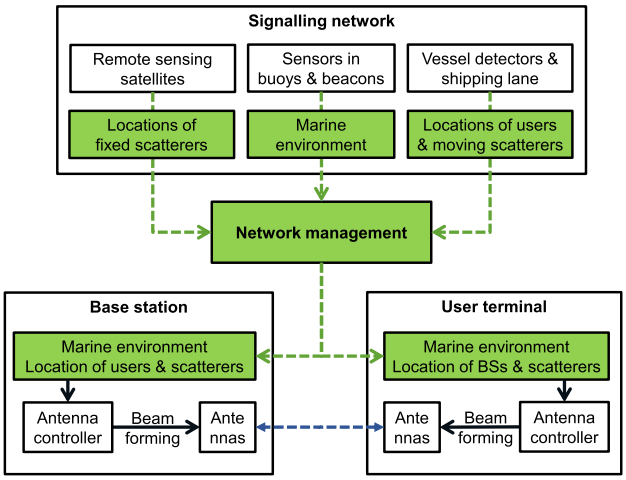

FIGURE 2. Illustration of an environment-aware MCN structure, where the information of marine environment (such as the locations of scatterers) is gathered and used for generating dynamic beams.

and $h_r^{(k)}$ represent the antenna heights above sea level of the i-th BS and the k-th MT, respectively, and $g\left(\theta_n^{(k,i)}\right)$ denotes the receiving antenna gain with respect to the azimuth angle between the k-th MT and the n-th CAA of the i-th BS.

In the following, we give an estimation of $\mathbf{T}^{(k,i)}$ using the geographic location information of scatterers. As maritime channels are discovered to have a limited number of scatterers, we adopt the widely-used geometric Saleh-Valenzuela channel model [16]. The number of scatterers is L_s, and each scatterer contributes a single propagation path between the BS and the MT. Under this model, the channel gain from the n-th CAA of the i-th BS to the k-th MT can be expressed as

$$\mathbf{H}_n^{(k,i)} = l_n^{(k,i)} \sum_{l=1}^{L_s} \alpha_{n,l}^{(k,i)} \mathbf{a}_{BS}\left(\varphi_{n,l}^{(k,i)}\right) \tag{7}$$

where $\alpha_{n,l}^{(k,i)} \sim \mathcal{CN}\left(0, \overline{P}_R\right)$ and $\varphi_{n,l}^{(k,i)}$ denote the complex gain and the AoD of the l-th path (as depicted in Fig. 1), respectively. Assuming uniform linear arrays are deployed at the BS and the antenna elements are closely packed at the MT, the m-th ($m = 1, 2, \ldots, M_k$) row of $\mathbf{a}_{BS}$ can be written as

$$\mathbf{a}_{BS}\left(\varphi_{n,l,m}^{(k,i)}\right) = \left[1, e^{j\frac{2\pi}{\lambda}d\sin\left(\varphi_{n,l}^{(k,i)}\right)}, \ldots, e^{j(L-1)\frac{2\pi}{\lambda}d\sin\left(\varphi_{n,l}^{(k,i)}\right)}\right] \tag{8}$$

TABLE 1. Geographic environment and channel parameters estimated.

Geographic Environment		Channel Parameters	
Location and antenna distribution of BSs	Location and antenna height of MTs	Path loss from BSs to MTs: $\mathbf{L}^{(k,i)}$	
	Location and attitude of satellites and STs	Antenna directivity of STs: $\theta_n^{(j,i)}$	Path loss from BSs to STs: $\mathbf{L}^{(j,i)}$
	Location of scatterers on the sea	AoD of each propagation path: $\varphi_{n,l}^{(k,i)}$ and $\varphi_{n,l}^{(j,i)}$	Antenna correlation: $\mathbf{T}^{(k,i)}$ and $\mathbf{T}^{(j,i)}$

where d is the distance between antenna elements. The channel covariance matrix can thus be expressed in (9), as shown at the bottom of this page.

Therefore, $\mathbf{T}_n^{(k,i)} \in \mathcal{C}^{L\times L}$ is estimated to be the normalized form of $\mathbf{R}_n^{(k,i)}$, i.e., $\mathbf{T}_n^{(k,i)} = \mathbf{R}_n^{(k,i)}/L_s\overline{P}_R M_k {l_n^{(k,i)}}^2$, and we have

$$\mathbf{T}^{(k,i)} = diag\left\{\mathbf{T}_1^{(k,i)}, \ldots, \mathbf{T}_{N_i}^{(k,i)}\right\}. \tag{10}$$

The total covariance of the interference plus noise at the j-th ($j = 1, 2, \ldots, J$) ST can be expressed as

$$\sigma_j^2(\mathbf{\Phi}) = \sum_{i=1}^{K} tr(\mathbf{L}^{(j,i)}\mathbf{T}^{(j,i)}\mathbf{L}^{(j,i)}\mathbf{\Phi}^{(i)}) + \sigma^2 \tag{11}$$

where $\mathbf{L}^{(j,i)}$ and $\mathbf{T}^{(j,i)}$ are the path loss and the transmit antenna correlation from the i-th BS to the j-th ST, respectively. To better evaluate this interference, the space environment information is used. Particularly, assuming the antennas of a ST are always pointing to the satellite, the antenna directivity $\theta_n^{(j,i)}$ can be estimated from the satellite's position (as depicted in Fig. 1), and $\mathbf{L}^{(j,i)}$ can be calculated according to (6). In addition, the AoD of each scattering path from the n-th CAA of the i-th BS to the j-th ST $\varphi_{n,l}^{(j,i)}$ can be obtained from the locations of scatterers, and $\mathbf{T}^{(j,i)}$ can be estimated accordingly.

In Table 1, we summarize the aforementioned environmental information on the sea and in space, as well as the channel parameters estimated from these information.

III. COOPERATIVE COVERAGE OPTIMIZATION

In this section, we optimize the coverage performance of the MCN using the aforementioned channel parameters estimated from the environmental information. Our objective is

$$\begin{aligned}\mathbf{R}_n^{(k,i)} &= \mathbb{E}\left[\mathbf{H}_n^{(k,i)H}\mathbf{H}_n^{(k,i)}\right] \\ &= \overline{P}_R M_k {l_n^{(k,i)}}^2 \\ &\cdot \begin{pmatrix} L_s & \cdots & \sum_{l=1}^{L_s} e^{-j(L-1)\frac{2\pi}{\lambda}d\sin\left(\varphi_{n,l}^{(k,i)}\right)} \\ \vdots & \ddots & \vdots \\ \sum_{l=1}^{L_s} e^{j(L-1)\frac{2\pi}{\lambda}d\sin\left(\varphi_{n,l}^{(k,i)}\right)} & \cdots & L_s \end{pmatrix}.\end{aligned} \tag{9}$$

to maximize the ergodic sum capacity for the MTs within the coverage by optimizing the precoding matrix cooperatively, while providing the STs with guaranteed QoS. The ergodic sum capacity can be written as

$$C\left(\mathbf{\Phi}\right)=\sum_{k=1}^{K}E\left[\log_2\det\left(\mathbf{I}_{M_k}+\frac{\mathbf{H}^{(k,k)}\mathbf{\Phi}^{(k)}\mathbf{H}^{(k,k)^H}}{\sigma_k^2\left(\mathbf{\Phi}\right)}\right)\right] \quad (12)$$

where $\mathbf{\Phi}=diag\left\{\mathbf{\Phi}^{(1)},\ \ldots,\ \mathbf{\Phi}^{(K)}\right\}$, and

$$\sigma_k^2\left(\mathbf{\Phi}\right)=\sum_{i=1,i\neq k}^{K}tr(\mathbf{L}^{(k,i)}\mathbf{T}^{(k,i)}\mathbf{L}^{(k,i)}\mathbf{\Phi}^{(i)})+\sigma^2 \quad (13)$$

is the total covariance of the interference plus noise at the k-th MT. The optimization problem is formulated as

$$\begin{aligned}
\max_{\left\{\mathbf{\Phi}^{(k)}|k=1,\ldots,K\right\}}\quad & C\left(\mathbf{\Phi}\right) && (14a)\\
s.t.\quad & tr(\mathbf{\Phi}^{(k)})\leq P_{\max}^{(k)} && (14b)\\
& \mathbf{\Phi}^{(k)}\geq 0 && (14c)\\
& \sigma_j^2\left(\mathbf{\Phi}\right)\leq\sigma_{\max}^{(j)} && (14d)\\
& \mathbf{\Phi}^{(k)}=\mathbf{w}^{(k)}\mathbf{b}^{(k)}\mathbf{b}^{(k)^H}\mathbf{w}^{(k)^H} && (14e)\\
& \left|\left[\mathbf{w}^{(k)}\right]_{(p,q)}\right|=\frac{1}{\sqrt{N_kL}} && (14f)
\end{aligned}$$

where $\sigma_{\max}^{(j)}$ denotes the interference threshold of the j-th ST.

There are three major challenges of solving the optimization problem. Firstly, to optimize $\mathbf{\Phi}$ with only the path loss $\left\{\mathbf{L}^{(k,i)}|k,i=1,2,\ldots,K\right\}$ and the transmit antenna correlation $\left\{\mathbf{T}^{(k,i)}|k,i=1,2,\ldots,K\right\}$, we have to calculate the expectation over the instantaneous sum capacity with respect to the small-scale fading $\left\{\mathbf{S}^{(k,i)}|k,i=1,2,\ldots,K\right\}$, and it is difficult to express $C\left(\mathbf{\Phi}\right)$ straightly without the expectation operator. Secondly, due to the mutual coupling of interference as shown in (11) and (13), $C\left(\mathbf{\Phi}\right)$ is not a concave function of $\mathbf{\Phi}$, and (14) is a complicated non-convex problem. Thirdly, $\mathbf{\Phi}^{(k)}$ is a function of $\mathbf{w}^{(k)}$ and $\mathbf{b}^{(k)}$ subject to (14e) and (14f), and it is intractable to obtain the optimal value of the coupled variables $\mathbf{\Phi}^{(k)}$, $\mathbf{w}^{(k)}$, and $\mathbf{b}^{(k)}$.

To tackle the first challenge, we adopt the random matrix theory and introduce an upper bound of $C\left(\mathbf{\Phi}\right)$, which is proved to be tight in the low signal-to-noise ratio (SNR) regime [15]. Defining $\mathbf{\Lambda}^{(k)}=\mathbf{L}^{(k,k)}\mathbf{T}^{(k,k)}\mathbf{L}^{(k,k)}$ $(k=1,\ldots,K)$, we can express the upper bound as

$$C_{ub}\left(\mathbf{\Phi}\right)=\xi_1\left(\mathbf{\Phi}\right)-\xi_2\left(\mathbf{\Phi}\right) \quad (15)$$

where both

$$\xi_1\left(\mathbf{\Phi}\right)=\sum_{k=1}^{K}\log_2\det\left(\sigma_k^2\left(\mathbf{\Phi}\right)\mathbf{I}_{N_kL_k}+M_k\mathbf{\Phi}^{(k)}\mathbf{\Lambda}^{(k)}\right) \quad (16)$$

and

$$\xi_2\left(\mathbf{\Phi}\right)=\sum_{k=1}^{K}N_kL_k\log_2\sigma_k^2\left(\mathbf{\Phi}\right) \quad (17)$$

are concave functions of $\mathbf{\Phi}$.

It should be noted that $C\left(\mathbf{\Phi}\right)$ is still a non-concave function of $\mathbf{\Phi}$. To transform (14) into a convex problem, we have to replace $\xi_2\left(\mathbf{\Phi}\right)$ with a linear function of $\mathbf{\Phi}$. To this end, we use the first-order Taylor expansion to approximate $\xi_2\left(\mathbf{\Phi}\right)$, and propose an iterative algorithm to solve (14) by solving a convex subproblem in each iteration.

At a certain point $\bar{\mathbf{\Phi}}$, the first-order Taylor expansion of $\xi_2\left(\mathbf{\Phi}\right)$ can be expressed as

$$\begin{aligned}
\hat{\xi}_2\left(\mathbf{\Phi}\,|\bar{\mathbf{\Phi}}\right)=&\sum_{k=1}^{K}N_kL_k\log_2\left(\sigma_k^2\left(\mathbf{\Phi}\right)\right)\\
&+\log_2\left(e\right)\sum_{k=1}^{K}\frac{N_kL_k}{\sigma_k^2\left(\bar{\mathbf{\Phi}}\right)}tr\left(\mathbf{\Pi}_k\left[\mathbf{\Phi}-\bar{\mathbf{\Phi}}\right]\right) \quad (18)
\end{aligned}$$

where

$$\mathbf{\Pi}^{(k,i)}=\begin{cases}\mathbf{L}^{(k,i)}\mathbf{T}^{(k,i)}\mathbf{L}^{(k,i)}, & k\neq i,\ k,i=1,\ldots,K\\ \mathbf{O}, & k=i=1,\ldots,K\end{cases} \quad (19)$$

and $\mathbf{\Phi}=diag\left\{\mathbf{\Phi}^{(1)},\ \ldots,\ \mathbf{\Phi}^{(K)}\right\}$. $C_{ub}\left(\mathbf{\Phi}\right)$ can thus be approximated as

$$C_{sub}\left(\mathbf{\Phi}\,|\bar{\mathbf{\Phi}}\right)=\xi_1\left(\mathbf{\Phi}\right)-\hat{\xi}_2\left(\mathbf{\Phi}\,|\bar{\mathbf{\Phi}}\right) \quad (20)$$

where $\hat{\xi}_2$ is a linear function of $\mathbf{\Phi}$, and $C_{sub}\left(\mathbf{\Phi}\,|\bar{\mathbf{\Phi}}\right)$ is a concave function of $\mathbf{\Phi}$. Therefore, the original problem (14) can be solved iteratively. The subproblem solved in each iteration s is formulated as

$$\begin{aligned}
\max_{\left\{\mathbf{\Phi}^{(k)}|k=1,\ldots,K\right\}}\quad & C_{sub}\left(\mathbf{\Phi}\,|\mathbf{\Phi}_{s-1}\right) && (21a)\\
s.t.\quad & tr(\mathbf{\Phi}^{(k)})\leq P_{\max}^{(k)} && (21b)\\
& \mathbf{\Phi}^{(k)}\geq 0 && (21c)\\
& \sigma_j^2\left(\mathbf{\Phi}\right)\leq\sigma_{\max}^{(j)} && (21d)\\
& \mathbf{\Phi}^{(k)}=\mathbf{w}^{(k)}\mathbf{b}^{(k)}\mathbf{b}^{(k)^H}\mathbf{w}^{(k)^H} && (21e)\\
& \left|\left[\mathbf{w}^{(k)}\right]_{(p,q)}\right|=\frac{1}{\sqrt{N_kL}}. && (21f)
\end{aligned}$$

To solve (21) in each iteration, we have to further decouple the variables $\mathbf{\Phi}^{(k)}$, $\mathbf{b}^{(k)}$, and $\mathbf{w}^{(k)}$. It is noted that by optimizing $\mathbf{\Phi}^{(k)}$, we actually provide a digital precoding scheme for the BSs, while a hybrid precoding scheme is obtained by optimizing $\mathbf{b}^{(k)}$ and $\mathbf{w}^{(k)}$. Inspired by this, we first obtain the optimal solution of $\mathbf{\Phi}^{(k)}$ by solving (21a)–(21d), which is a convex problem. Then, sub-optimal solutions of $\mathbf{b}^{(k)}$ and $\mathbf{w}^{(k)}$ can be obtained from $\mathbf{\Phi}^{(k)}$ by solving the following optimization problem [17]:

$$\begin{aligned}
\min_{\mathbf{b}^{(k)},\mathbf{w}^{(k)}}\quad & \left\|\mathbf{\Phi}^{(k)}-\mathbf{b}^{(k)}\mathbf{w}^{(k)}\mathbf{w}^{(k)^H}\mathbf{b}^{(k)^H}\right\| && (22a)\\
s.t.\quad & \left|\left[\mathbf{w}^{(k)}\right]_{(p,q)}\right|=\frac{1}{\sqrt{N_kL}}. && (22b)
\end{aligned}$$

The proposed algorithm is described in detail in Algorithm 1. In practical MCNs where large antenna arrays are equipped at the BSs, hybrid precoding can be used instead of full digital precoding to reduce the hardware cost and complexity by reducing the number of RF chains. Therefore,

Algorithm 1 Iterative Optimization of Input Covariance and Precoding Matrix

1: Initially set $s = 0$, $S_{max} = 10$, $\delta = 10^{-3}$.
2: Initialize $\mathbf{\Phi}$ with a uniform power distribution, i.e., $\mathbf{\Phi}_0 = diag\left\{\mathbf{\Phi}_0^{(1)}, \ldots, \mathbf{\Phi}_0^{(K)}\right\}$ with $\mathbf{\Phi}_0^{(k)} = \frac{P_{\max}^{(k)}}{N_k L_k}\mathbf{I}$.
3: **repeat**
4: Update $s = s + 1$.
5: Solve the subproblem (21a)–(21d) and obtain the optimal input covariances $\mathbf{\Phi}_s^{(k)}$, $k = 1, \ldots, K$.
6: Set $\mathbf{\Phi}_s = diag\left\{\mathbf{\Phi}_s^{(1)}, \ldots, \mathbf{\Phi}_s^{(K)}\right\}$.
7: **until** $\frac{C_{sub}(\mathbf{\Phi}_s) - C_{sub}(\mathbf{\Phi}_{s-1})}{C_{sub}(\mathbf{\Phi}_{s-1})} < \delta$ or $s = S_{\max}$.
8: Solve (22) and obtain the suboptimal precoding matrixes $\mathbf{b}^{(k)}$ and $\mathbf{w}^{(k)}$ if hybrid precoding is used.

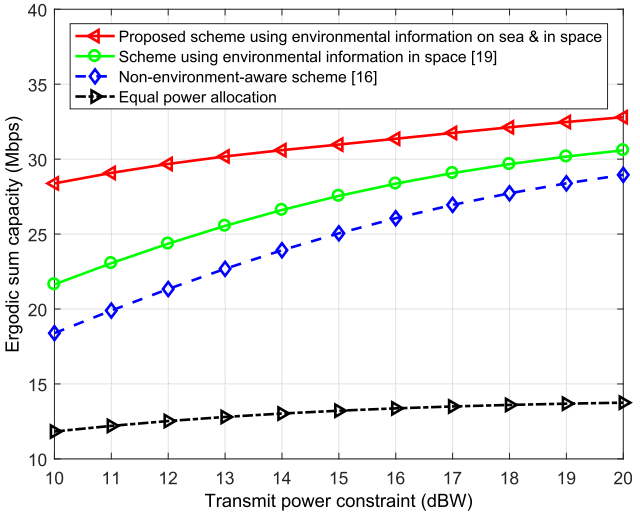

FIGURE 3. Ergodic sum capacity using different schemes.

both the input covariances and the precoding matrixes are optimized to adapt to different scenarios.

IV. PERFORMANCE EVALUATION AND DISCUSSIONS

The MCN simulated below consists of 3 onshore BSs, 3 MTs and 2 STs within 50 km offshore. We assume $N_k = 3$, $L = 3$ and $M_k = 2$ for all k ($k = 1, 2, \ldots, K$), and $M_j = 1$ for all j ($j = 1, 2, \ldots, J$). The carrier frequency and the bandwidth are set to be 1.9 GHz and 20 MHz, respectively. The transmit and receive antenna heights are assumed to be 50 m and 10 m, respectively. The noise power density is -174 dBm/Hz. The receiving antenna gain is given as

$$g\left(\theta_n^{(k,i)}\right) = g(0) \cdot 20^{-\frac{12\theta_n^{(k,i)}/\theta_{\text{th}}}{20}} \tag{23}$$

where $g(0)$ is the boresight gain, and θ_{th} is the angle between -3 dB points of the main lobe [18].

First, we evaluate the ergodic sum capacity under different transmit power constraints. We compare the performance of the proposed environment-aware scheme with that of the space-environment-aware scheme in [19], the non-environment-aware scheme in [15], and the equal power allocation scheme as $\mathbf{\Phi}^{(k)} = \frac{P_{\max}^{(k)}}{N_k L_k}\mathbf{I}$. As shown in Fig. 3, the proposed scheme achieves larger ergodic sum capacity than the other schemes. Using the environmental information in space, [19] outperforms the non-environment-aware scheme and the equal power allocation scheme, due to the use of directional antennas at the transmitter/receiver. Furthermore, the performance gap can be greatly enlarged for maritime communications using the proposed scheme. The performance gain mainly comes from the utilization of marine environment information, i.e., the location and mobility information of scatterers. With the knowledge of transmit antenna correlation derived from the above information, the proposed scheme both enhances the desired signal and mitigates the co-channel interference.

The shore-based MCN has to cover a vast area with a limited number of BS sites. It usually adopts high-powered

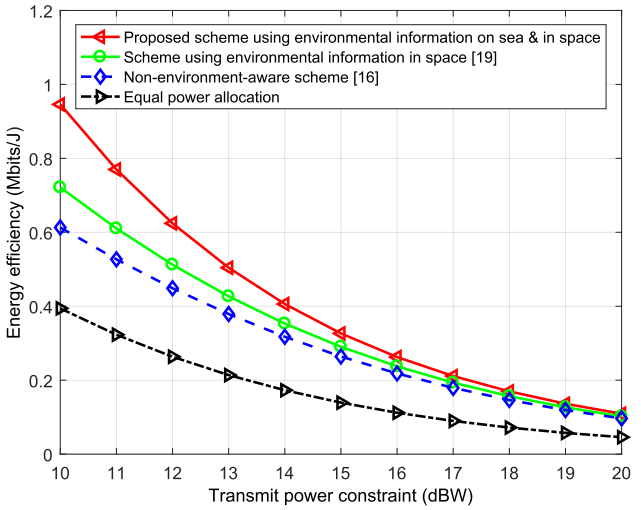

FIGURE 4. Energy efficiency using different schemes.

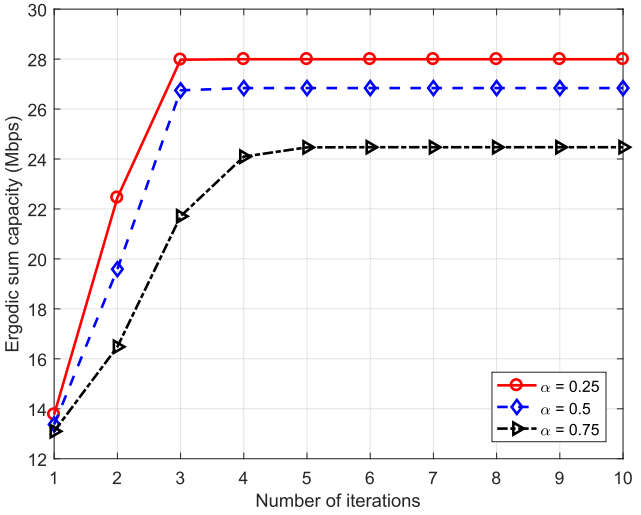

FIGURE 5. Algorithm convergence with different transmit antenna correlation.

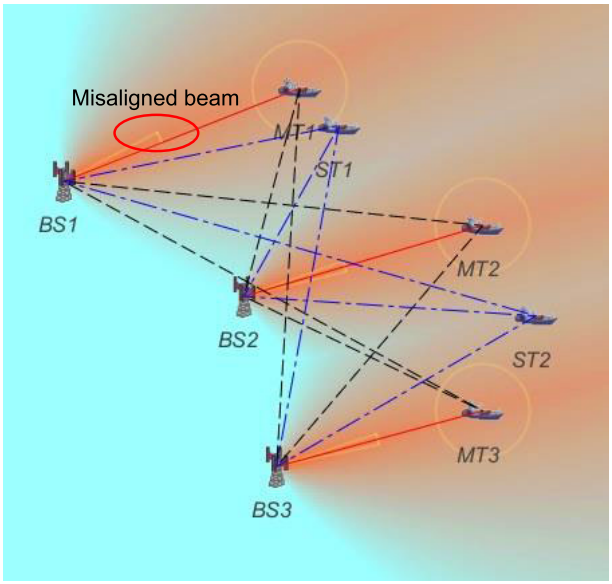

(a) Single-beam transmit antenna.

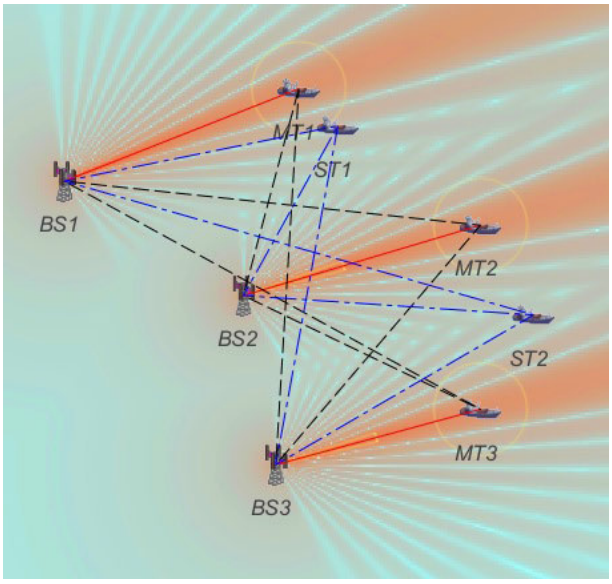

(b) Phased-array transmit antennas.

FIGURE 6. The SINR of MTs within the coverage area of the MCN (with a resolution of 1 km).

BSs for remote transmission, resulting in low energy efficiency. Besides, previous studies have suggested that energy efficiency can be severely degraded by the strong co-channel interference, and there is a tradeoff between energy efficiency and spectral efficiency [20]– [23]. For this reason, we simulate the energy efficiency using different schemes in Fig. 4. It can be seen that the proposed environment-aware scheme achieves higher energy efficiency than the non-environment-aware schemes, although it aims to maximize the ergodic sum capacity. On the other hand, the energy efficiency decreases with the increase of $P_{\max}^{(k)}$, as the Shannon capacity grows logarithmically with the signal-to-interference-plus-noise ratio (SINR), and a larger value of $P_{\max}^{(k)}$ leads to stronger interference.

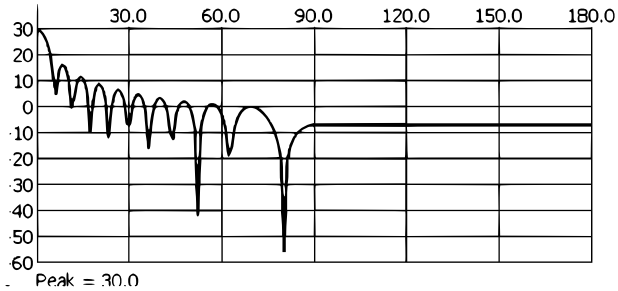

(a) Traditional Bessel beams.

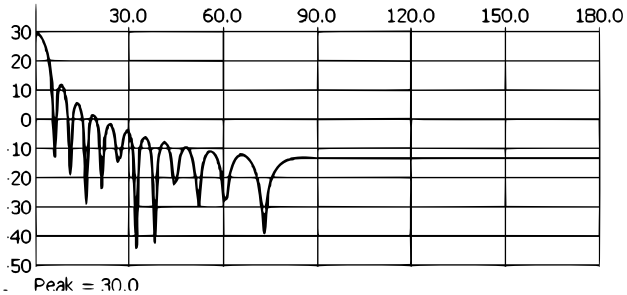

(b) Dynamic beams with sidelobe suppression.

FIGURE 7. Radiation pattern of phased array antennas. The figures are obtained from Visualyse Professional 7 [24], but converted into vector format to improve visibility.

Fig. 5 depicts the convergence process of Algorithm 1, where $0 \leq \alpha_{kn} \leq 1$ denotes the transmit antenna correlation coefficient, and a larger value of α implies higher correlation. We can observe that the ergodic sum capacity converges within 10 iteration steps for $\alpha = 0.25$, 0.5 and 0.75. The relatively fast convergence speed of the iterative algorithm proves the feasibility of the scheme in real MCNs.

Further, we evaluate the coverage performance of the proposed scheme using Visualyse Professional 7, where the real-world geographic information of a coastal area around the Chongming Island of China is used for simulation [24]. Fig. 6 shows the SINR of a MT moving within the area, where directional transmit antennas and omnidirectional receive antennas are used. It can be observed that the proposed scheme can achieve dynamic coverage by both enhancing the desired signal and mitigating the co-channel interference. Specifically, we compare the performance when a single-beam transmit antenna (i.e. $L = 1$) and phased-array transmit antennas are equipped at the BS. As can be seen in Fig. 6(a), the beam generated by BS 1 does not strictly point to MT 1. Instead, it has to be misaligned to avoid interfering with ST 1, which will inevitably reduce the SINR of MT 1.

The use of phased-array antennas can address this issue to some extent. As depicted in Fig. 6(b) and Fig. 7, the sidelobes of the beam are suppressed to mitigate the co-channel interference to certain angles, while the mainlobe of the beam can still point to the desired direction to maximize the SINR of the MT. In other words, with phased-array antennas equipped at the BS, the transmit antenna correlation derived from marine environment information can be utilized to achieve better coverage performance.

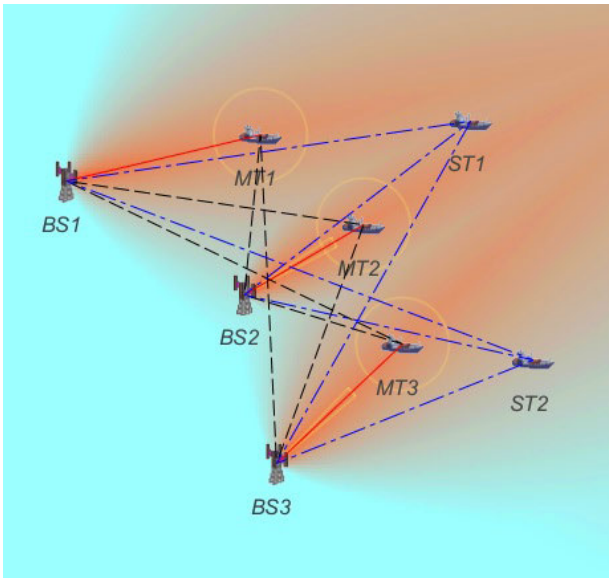

(a) When STs are farther offshore than MTs.

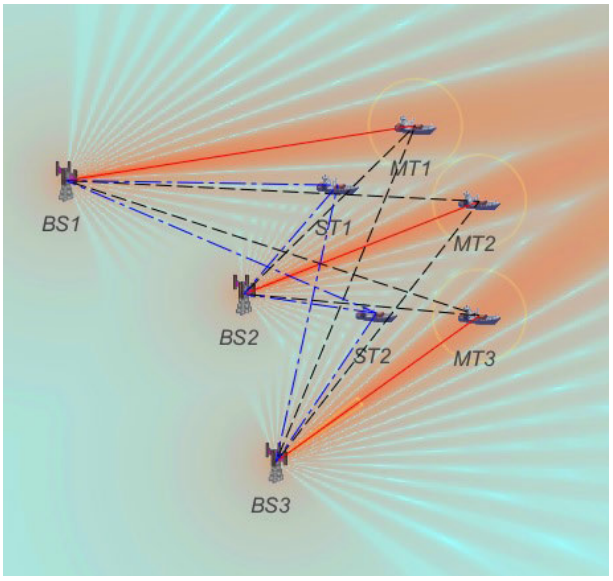

(b) When MTs are farther offshore than STs.

FIGURE 8. Illustration of dynamic coverage optimization for different network topologies.

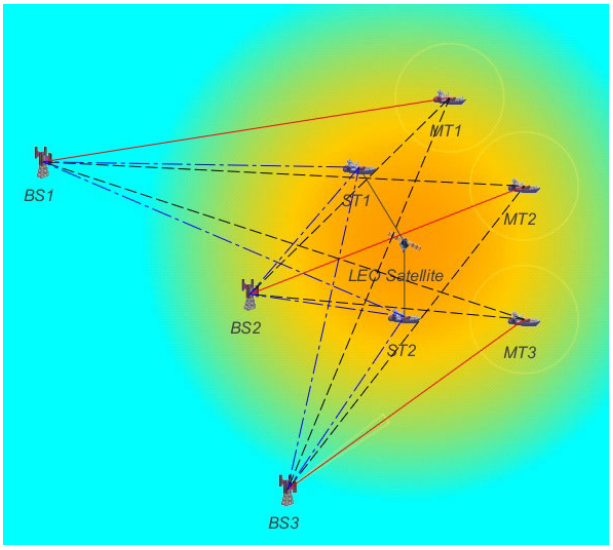

(a) Coverage performance of the maritime satellite.

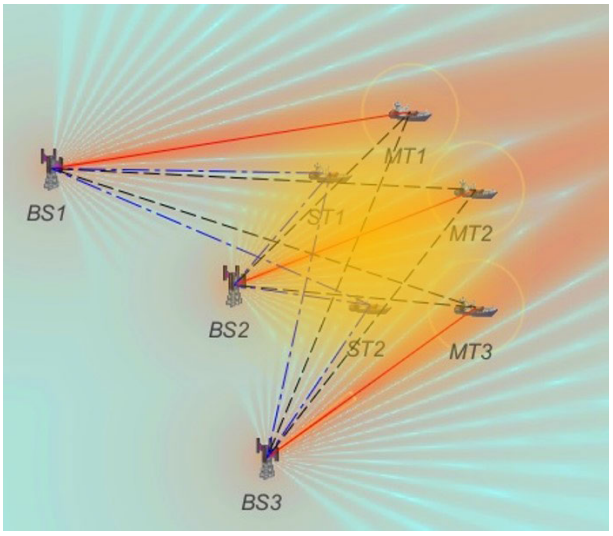

(b) Coverage performance of the space-ground integrated MCN.

FIGURE 9. Overall evaluation of the coverage performance.

In traditional scenarios, shore-based MCNs mainly cover offshore areas, while maritime satellites serve the users farther away. However, MTs can be farther offshore than STs in extreme cases. As depicted in Fig. 8, the proposed dynamic coverage optimization scheme also has good performance for this network topology. Indeed, as shown in Fig. 8(b), if BS 2 serves ST 2 (which is nearer than MT 2), it will inevitably interfere with MT 3. Therefore, it is better for BS 2 to serve MT 2, leaving ST 2 to the satellites. In Fig. 9, we give an overall evaluation of the coverage performance of the space-ground integrated MCN. It can be observed that the shore-based MCN and the maritime satellite are complementary in terms of coverage areas when working in a coordinated way. In other words, the proposed scheme can break the boundaries between the coverage areas of shore-based MCNs and maritime satellites, and achieve dynamic coverage for different network topologies. It is different from traditional scenarios where shore-based MCNs and satellites cover offshore areas and areas farther away from the coast, respectively.

V. CONCLUSION

In this paper, we have exploited the marine environment information for coverage optimization in the space-ground integrated MCN. Particularly, the location and mobility information of scatterers on the sea have been utilized to estimate the transmit antenna correlation. On that basis, we have formulated a non-convex problem for the optimization of input covariances and precoding matrixes, to maximize the ergodic sum capacity for the MTs while providing the STs with

guaranteed QoS. We have introduced a tight upper bound of the ergodic sum capacity, and proposed an iterative algorithm to solve the problem by solving a convex subproblem in each iteration. Simulation results have shown that the proposed scheme can significantly improve the ergodic sum capacity compared with existing approaches. Besides, it can break the boundaries between the coverage areas of shore-based MCNs and maritime satellites, achieving dynamic coverage for different network topologies. We have further pointed out that, the performance gain mainly comes from the utilization of marine environment information, which implies a brand new way for coverage optimization in practical MCNs.

REFERENCES

[1] Y. Xu, "Quality of service provisions for maritime communications based on cellular networks," *IEEE Access*, vol. 5, pp. 23881–23890, 2017.

[2] P. J. Hadinger, "Inmarsat global Xpress the design, implementation, and activation of a global Ka-band network," in *Proc. AIAA Int. Commun. Satell. Syst. Conf.*, QLD, Australia, Sep. 2015, pp. 1–8.

[3] H. Seo, J. Shim, S. Ha, Y.-S. Kim, and J. Jeong, "Ultra long range LTE ocean coverage solution," in *Proc. 24th Int. Conf. Telecommun. (ICT)*, Limassol, Cyprus, May 2017, pp. 1–5.

[4] A. Kapovits, M.-I. Corici, I.-D. Gheorghe-Pop, A. Gavras, F. Burkhardt, T. Schlichter, and S. Covaci, "Satellite communications integration with terrestrial networks," *China Commun.*, vol. 15, no. 8, pp. 22–38, Aug. 2018.

[5] T. Wei, W. Feng, Y. Chen, C.-X. Wang, N. Ge, and J. Lu, "Hybrid satellite-terrestrial communication networks for the maritime Internet of Things: Key technologies, opportunities, and challenges," Mar. 2019, *arXiv:1903.11814*. [Online]. Available: http://arxiv.org/abs/1903.11814

[6] X. Li, W. Feng, Y. Chen, C.-X. Wang, and N. Ge, "Maritime coverage enhancement using UAVs coordinated with hybrid satellite-terrestrial networks," *IEEE Trans. Commun.*, vol. 68, no. 4, pp. 2355–2369, Apr. 2020.

[7] S. Vuppala, M. Sellathurai, and S. Chatzinotas, "Optimal deployment of base stations in cognitive satellite-terrestrial networks," in *Proc. Intern. ITG Workshop Smart Antennas*, Bochum, Germany, Mar. 2018, pp. 1–8.

[8] M. Jia, X. Zhang, X. Gu, and Q. Guo, "Energy efficient cognitive spectrum sharing scheme based on inter-cell fairness for integrated satellite-terrestrial communication systems," in *Proc. IEEE 87th Veh. Technol. Conf. (VTC Spring)*, Porto, Portugal, Jun. 2018, pp. 1–6.

[9] Y.-W. Jiang, J. Ouyang, C.-Y. Yin, Z.-Y. Xu, X.-S. Tao, and L. Lou, "Downlink beamforming scheme for hybrid satellite–terrestrial networks," *IET Commun.*, vol. 12, no. 18, pp. 2342–2346, Nov. 2018.

[10] W. Feng, N. Ge, and J. Lu, "Coordinated satellite-terrestrial networks: A robust spectrum sharing perspective," in *Proc. 26th Wireless Opt. Commun. Conf. (WOCC)*, Newark, NJ, USA, Apr. 2017, pp. 1–5.

[11] J. Wang, H. Zhou, Y. Li, Q. Sun, Y. Wu, S. Jin, T. Q. S. Quek, and C. Xu, "Wireless channel models for maritime communications," *IEEE Access*, vol. 6, pp. 68070–68088, 2018.

[12] C. Liu, W. Feng, T. Wei, and N. Ge, "Fairness-oriented hybrid precoding for massive MIMO maritime downlink systems with large-scale CSIT," *China Commun.*, vol. 15, no. 1, pp. 52–61, Jan. 2018.

[13] M. Stasolla, J. J. Mallorqui, G. Margarit, C. Santamaria, and N. Walker, "A comparative study of operational vessel detectors for maritime surveillance using satellite-borne synthetic aperture radar," *IEEE J. Sel. Topics Appl. Earth Observ. Remote Sens.*, vol. 9, no. 6, pp. 2687–2701, Jun. 2016.

[14] T. Wei, W. Feng, J. Wang, N. Ge, and J. Lu, "Exploiting the shipping lane information for energy-efficient maritime communications," *IEEE Trans. Veh. Technol.*, vol. 68, no. 7, pp. 7204–7208, Jul. 2019.

[15] W. Feng, Y. Wang, N. Ge, J. Lu, and J. Zhang, "Virtual MIMO in multi-cell distributed antenna systems: Coordinated transmissions with large-scale CSIT," *IEEE J. Sel. Areas Commun.*, vol. 31, no. 10, pp. 2067–2081, Oct. 2013.

[16] R. He, B. Ai, A. F. Molisch, G. L. Stuber, Q. Li, Z. Zhong, and J. Yu, "Clustering enabled wireless channel modeling using big data algorithms," *IEEE Commun. Mag.*, vol. 56, no. 5, pp. 177–183, May 2018.

[17] Z. Zhou, N. Ge, Z. Wang, and S. Chen, "Hardware-efficient hybrid precoding for millimeter wave systems with multi-feed reflectarrays," *IEEE Access*, vol. 6, pp. 6795–6806, 2018.

[18] C.-W. Ang and S. Wen, "Signal strength sensitivity and its effects on routing in maritime wireless networks," in *Proc. 33rd IEEE Conf. Local Comput. Netw. (LCN)*, Montreal, QC, Canada, Oct. 2008, pp. 192–199.

[19] T. Xia, M. M. Wang, and X. You, "Satellite machine-type communication for maritime Internet of Things: An interference perspective," *IEEE Access*, vol. 7, pp. 76404–76415, 2019.

[20] Z. Zhou, M. Dong, K. Ota, G. Wang, and L. T. Yang, "Energy-efficient resource allocation for D2D communications underlaying Cloud-RAN-Based LTE—A networks," *IEEE Internet Things J.*, vol. 3, no. 3, pp. 428–438, Jun. 2016.

[21] Z. Zhou, M. Dong, K. Ota, J. Wu, and T. Sato, "Energy efficiency and spectral efficiency tradeoff in Device-to-Device (D2D) communications," *IEEE Wireless Commun. Lett.*, vol. 3, no. 5, pp. 485–488, Oct. 2014.

[22] Z. Zhou, C. Zhang, J. Wang, B. Gu, S. Mumtaz, J. Rodriguez, and X. Zhao, "Energy-efficient resource allocation for energy harvesting-based cognitive Machine-to-Machine communications," *IEEE Trans. Cognit. Commun. Netw.*, vol. 5, no. 3, pp. 595–607, Sep. 2019.

[23] Z. Zhou, J. Feng, Z. Chang, and X. Shen, "Energy-efficient edge computing service provisioning for vehicular networks: A consensus ADMM approach," *IEEE Trans. Veh. Technol.*, vol. 68, no. 5, pp. 5087–5099, May 2019.

[24] (2020). *Transfinite Systems: Visualyse Professional–Make Life Easier, Improve Your Output*. Accessed: Feb. 11, 2020. [Online]. Available: https://www.transfinite.com/content/professional

TE WEI (Student Member, IEEE) received the B.S. degree from the Department of Electronic Engineering, Tsinghua University, Beijing, China, in 2014, where he is currently pursuing the Ph.D. degree. His current research interests include performance analysis and resource allocation for maritime broadband communication networks.

WEI FENG (Senior Member, IEEE) received the B.S. and Ph.D. degrees from the Department of Electronic Engineering, Tsinghua University, Beijing, China, in 2005 and 2010, respectively. He is currently an Associate Professor with the Department of Electronic Engineering, Tsinghua University. His research interests include maritime communication networks, largescale distributed antenna systems, and coordinated satellite-UAV-terrestrial networks. He serves as the Assistant to the Editor-in-Chief for *China Communications*, an Editor for the IEEE TRANSACTIONS ON COGNITIVE COMMUNICATIONS AND NETWORKING, and an Associate Editor for IEEE ACCESS.

NING GE (Member, IEEE) received the B.S. and Ph.D. degrees from Tsinghua University, Beijing, China, in 1993 and 1997, respectively. From 1998 to 2000, he was with ADC Telecommunications, Dallas, TX, USA, where he researched the development of ATM switch fabric ASIC. Since 2000, he has been with the Department of Electronics Engineering, Tsinghua University, where he is currently a Professor and the Director of the Communication Institute. He has published over 100 articles. His current research interests include communication ASIC design, short range wireless communications, and wireless communications. He is a Senior Member of CIC and CIE.

JIANHUA LU (Fellow, IEEE) received the B.S.E.E. and M.S.E.E. degrees from Tsinghua University, Beijing, China, in 1986 and 1989, respectively, and the Ph.D. degree in electrical and electronic engineering from The Hong Kong University of Science and Technology, Hong Kong, in 1998.

Since 1989, he has been with the Department of Electronic Engineering, Tsinghua University, where he is currently a Professor. He was granted funding as a National Distinguished Young Scholar, and headed the Innovative Research Group of the National Natural Science Foundation of China. He was a Chief Scientist of the National Basic Research Program (973) of China. He has made influential contributions to China's national major engineering programs, such as the Lunar Program. He has published over 300 technical articles in international journals and conference proceedings. His current research interests include broadband wireless communications, multimedia signal processing, and satellite communications.

Dr. Lu is a member of the Chinese Academy of Sciences. He also serves as an Executive Member of the Council of Chinese Institute of Electronics. He has been an Active Member of professional societies. He served in numerous IEEE conferences as a member of Technical Program Committees. He was a recipient of the Best Paper Awards at the IEEE International Conference on Communications, Circuits, and Systems 2002, the China Communications 2006, the IEEE Embedded-Com 2012, the Second Prize of National Technical Innovation Award twice, and the Second Prize of National Natural Science Award of China. He was honored as the Yangtze River Scholar Distinguished Professor. He was the Lead Chair of the General Symposium of IEEE ICC 2008, as well as a Program Committee Co-Chair of the 9th IEEE International Conference on Cognitive Informatics, in 2010, and the General Co-Chair of the 14th IEEE International Conference on Cognitive Informatics, in 2015. From 2008 to 2011, he was an Editor of the IEEE TRANSACTIONS ON WIRELESS COMMUNICATIONS.